International Journal of Nanomedicine

Dovepress
Taylor & Francis Group

Open Access Full Text Article

ORIGINAL RESEARCH

Iron-Oxide Labeled Stem Cells with Specific Magnetic Occurrence for Effective in Mouse Model of Cisplatin-Induced Acute Kidney Injury

Ke Wang[1,2,*], Ye Zhao[3,*], Huiying Lv[1], Xiuying Li[1]

[1]Scientific Research Center, China-Japan Union Hospital of Jilin University, Changchun, Jilin, People's Republic of China; [2]Gynecology and Obstetrics Department, China-Japan Union Hospital of Jilin University, Changchun, Jilin, People's Republic of China; [3]Dermatological Department, China-Japan Union Hospital of Jilin University, Changchun, Jilin, People's Republic of China

*These authors contributed equally to this work

Correspondence: Xiuying Li, Email lixiuying@jlu.edu.cn

Background: Acute kidney injury (AKI) is characterized by the abrupt loss of renal function and lack of curative therapies. Placental-derived mesenchymal stem cells (PL-MSCs) have shown promise in regenerative medicine, including in the treatment of AKI. However, optimizing the therapeutic effects of PL-MSCs remains a critical objective. Magnetic targeting is one potential avenue of optimization. Using iron oxide-labeled MSCs with an external magnetic field to increase cell homing ability may be an ideal method for improving the cell therapy effects in vivo.

Methods: In this study, PL-MSCs were labeled with Fe_3O_4 nanoparticles coated with polydopamine (Fe_3O_4@PDA NPs) for 24 h, and cell efficiency and viability were tested. The conditionally immortalized mice renal tubular endothelial cells (mRTECs) were incubated with cisplatin (Cis) and co-cultured with non-labeled or NP-labeled MSCs. The protective effect of NP-labeled MSCs on mRTEC was evaluated. In in vivo experiments, non-labeled or NP-labeled MSCs, with or without an external magnetic field, were injected into mice with Cis-induced AKI. The blood and tissue samples were collected to assess renal function and tissue damage.

Results: The study confirmed that MSCs or MSC-NP can significantly improve Cis-induced mRTEC injury. In addition, NP-labeled MSCs with an external magnetic field (magnetically-targeted MSCs) improved their homing to the kidney tissues in mice with AKI, resulting in enhanced kidney function compared with those of mice treated with MSC or NP-labeled MSC treatment alone. Moreover, magnetically-targeted MSCs alleviated renal injury through suppressing oxidative stress and inflammation, reducing cell apoptosis, and promoting cell proliferation.

Conclusion: Magnetic targeting enhances the therapeutic effects of PL-MSCs on Cis-induced AKI in mice, suggesting that magnetically-targeted MSCs could serve as potential treatments for patients with Cis-induced AKI.

Keywords: acute kidney injury, cisplatin, placental-derived mesenchymal stem cells, inflammation, oxidative stress, apoptosis, proliferation

Introduction

Cisplatin (Cis) is a chemotherapeutic drug commonly used to treat various solid cancers globally.[1] However, its clinical application is often limited by serious adverse reactions involving various organs.[2–4] Approximately one-third of patients receiving Cis treatment may experience nephrotoxicity, including acute kidney injury (AKI).[5] Cis induces apoptosis, inflammatory response, and fibrosis in renal tubular epithelial cells.[6,7] Although treatments such as fluid management and continuous blood purification therapy are available, so far, no specific pharmacotherapy effectively treats for Cis-induced AKI.

Mesenchymal stem cells (MSCs) are a promising source of stem cells for tissue engineering and regenerative medicine. MSCs mainly exist in human bone marrow, skin, umbilical cord tissue, and adipose tissue.[8–10] Increasing experimental evidence suggests that MSCs can be used to ameliorate Cis-induced kidney injury and protect against tubular damage and renal dysfunction.[11–16] However, in several tissues, such as the bone marrow, MSC isolation is

Received: 17 March 2025
Accepted: 20 August 2025
Published: 18 September 2025

invasive and often requires multiple sampling to obtain sufficient quantities. Placental-derived MSCs (PL-MSCs) have been studied as promising tools for regenerative cell therapy. PL-MSCs are easily obtained after childbirth, have a high cell yield and strong proliferation ability, and, most importantly, can be safely applied owing to their low immunogenicity. PL-MSCs have greater expansion potential and possess greater immunomodulatory capacity than adult bone marrow MSCs.[17] The preclinical studies have shown that PL-MSCs secrete immunomodulatory and angiogenic cytokines which aid in healing and remodeling of tissue.[18] At present, PL-MSCs have been investigated in animal models for almost every disease imaginable, from multiple sclerosis and erectile dysfunction to coronavirus disease, chronic lung injury, and renal disease.[19–22] Thus, PL-MSCs may become a promising source for cell therapy of AKI. The therapeutic effects of MSCs largely depend on the number of MSCs that successfully reach the target site. After intravenous infusion, only a small portion of cells reach the target tissue, which indicates the low homing efficiency of MSCs. Therefore, identifying an effective cell delivery method that enhances cell homing to the target site is crucial.

The development of nanotechnology has introduced new methods to address public health problems. Magnetically-targeted delivery, which predominantly comprises magnetic particles, cargo, and carriers, is a new delivery technology that has recently become increasingly popular.[23–25] In magnetically-targeted delivery systems, carriers that respond to specific magnetic fields can be magnetically guided to the target site, increasing the concentration of the content at the target site while reducing toxicity and off-target side effects.[26] Currently, the most widely used type of magnetic carrier are Fe_3O_4 nanoparticles (Fe_3O_4 NPs), which exhibit magnetism, low toxicity, and high biocompatibility. Fe_3O_4 NPs have been widely validated for cancer treatment, whether as carriers for anticancer drugs for magnetically-targeted delivery or as thermal therapy agents to enhance the efficacy of chemotherapy drugs.[27–29] Fe_3O_4 NPs coated with polydopamine (Fe_3O_4@PDA NPs) exhibit enhanced superparamagnetism, better biocompatibility, and lower toxicity.[30] Fe_3O_4@PDA NPs are more appropriate carriers for clinical treatments. Labeling specific cells with Fe_3O_4@PDA NPs can increase the migration and distribution of cells from the blood to target sites in the kidney. As such, studies have shown that magnetically-targeted guided MSCs can be applied to repair other injuries, such as cartilage injury, spinal cord injury, and myocardial infarction.[31–33] In addition, a study has shown that magnetically-targeted PL- MSCs can maximize the therapeutic effect of glioma.[34]

The present study aimed to evaluate a non-invasive method to stimulate cell arrival at the injury site through labeling Fe_3O_4@PDA NPs, which promote the recruitment of MSCs to the site of injury in AKI mice, to enhance the regenerative ability of PL-MSCs. In addition, we evaluated the therapeutic effect when Fe_3O_4@PDA labeled MSCs were administered to a mouse AKI model.

Materials and Methods

Cell Culture

Human PL-MSCs were prepared as described previously.[35] All handling procedures were performed with the approval of the Research Ethics Committee of the China-Japan Union Hospital of Jilin University after informed written consent was obtained from the participants, in accordance with the Declaration of Helsinki. PL-MSCs were plated in 100-mm dishes containing α-minimum essential medium with 10% fetal bovine serum (FBS; Invitrogen Australia Pty. Ltd., Mount Waverley, Victoria, Australia). Conditionally immortalized mice renal tubular endothelial cells (mRTECs) were purchased from the Shanghai Institute of Cell Biology (Shanghai, China) and cultured in Roswell Park Memorial Institute 1640 medium (Gibco, Gaithersburg, MD, USA) containing 10% FBS. All cells were placed at 37 °C in a 5% CO_2 incubator.

The Preparation of Mesenchymal Stem Cells (MSCs) with Fe_3O_4 Coated with Polydopamine Nanoparticles

The synthesis and characterization of Fe_3O_4@PDA NPs was conducted as previously described.[36] PL-MSCs were cultured in six-well plates. When confluent, the medium was replaced, and concentrations in the range of 25 to 200 μg/mL of Fe_3O_4@PDA NPs were added to the medium and then incubated for 24 h. Excess NPs were eliminated by rinsing with phosphate-buffered saline (PBS).

Detection of Intracellular Iron via Prussian Blue Staining

PL-MSCs were cultured in six-well plates. When the confluence rate of the MSCs reached approximately 80%, different concentrations of NPs were added to the cell medium and incubated for 24 h. The MSCs labeled with NPs were fixed with 4% paraformaldehyde solution for 30 min and stained with a Prussian blue kit (Beijing Solarbio Science and Technology Co. Ltd., Beijing, China) in accordance with the manufacturer's instructions. The stained MSCs were observed under a microscope (CKX 41; Olympus, Tokyo, Japan).

Measurement of MSC Cytotoxicity and Proliferation After Labeling with Fe_3O_4 Coated with Polydopamine Nanoparticles

PL-MSCs were labeled with Fe_3O_4@PDA NPs at concentrations in the range of 25 to 200 μg/mL. After incubation for 24 h, the cell-counting kit 8 (CCK8) detection kit (Beyotime, Shanghai, China) was used to measure the activity of the cells. Alternatively, cells were washed with PBS after labeling with Fe_3O_4@PDA NPs, continued to cultivate for 7 d, and then evaluated for cell proliferation using the CCK8 assay. The Fe_3O_4@PDA NPs, which exhibited the lowest cytotoxicity, were used for subsequent experiments.

Detection of Intracellular Iron Using Transmission Electron Microscopy

PL-MSCs labeled with Fe_3O_4@PDA NPs were fixed in 2.5% glutaraldehyde overnight at 4 °C. After washing with PBS, the MSCs were post-fixed with 1% osmium tetroxide for 2 h. They were then dehydrated in graded ethanol solutions and examined using transmission electron microscopy (TEM) (HT7800; HITACHI, Chiyoda, Japan).

Identification of Stem Cell Characteristics in Nanoparticle-Labeled MSCs

PL-MSCs were labeled with Fe_3O_4@PDA NPs for 24 h. NP-labeled or unlabeled cells were incubated with antibodies against CD73, CD45, CD34, CD19, CD11b, CD90, HLA-DR, and CD105 (Beckman, Brea, CA, USA) and incubated in the absence of light for 30 min at 4 °C. The cells were analyzed by flow cytometry (FACScan; BD Biosciences, Franklin Lakes, NJ, USA). Cells were cultured with either adipogenic medium (StemPro® Adipogenesis Differentiation kit; Invitrogen, Carlsbad, CA, USA) for 21 d or osteogenic medium (StemPro® Osteogenesis Differentiation kit; Invitrogen, Carlsbad, CA, USA) for 28 d, with the medium changed every 3 d. Subsequently, the cells were stained with Oil Red O (Sigma-Aldrich, St. Louis, MO, USA) for adipogenic differentiation or Alizarin Red S (Alizarin Staining Kit; Genmed, Shanghai, China) for osteogenic differentiation. The cells were then observed under a light microscope (CKX 41; Olympus).

Indirect Co-Cultures of Cis-Stimulated Mice Renal Tubular Endothelial Cells and Nanoparticle-Labeled or Unlabeled MSCs

For in vitro treatments, mRTECs were treated with 2.5 μg/mL cisplatin (Cis, Sigma-Aldrich) for 6 h. Then the control and Cis groups were switched to normal medium. For the other two groups, after mRTECs were treated with 2.5 μg/mL Cis for 6 h, the NP-labeled or unlabeled MSCs were co-cultured in six-well Transwell plates for 24 h. For Transwell co-cultures, 2×10^5 MSCs were plated onto cell-culture inserts (24-mm well dimension, 0.4-μm pore membrane, Corning, Lowell, MA, USA), whereas 2×10^5 Cis-stimulated mRTECs were placed in the lower chambers of the six-well plates and cultured for 24 h. Three independent experiments were conducted for the in vitro co-culture experiments.

Detection of Apoptosis and Reactive Oxygen Species Levels via Flow Cytometric

A six-well plate containing mRTECs was treated with 2.5 μg/mL Cis for 6 h. After co-culturing of Cis-stimulated mRTECs with NP-labeled or unlabeled MSCs, mRTECs were washed, resuspended in binding buffer, and stained with Annexin V/PI (Beyotime) for apoptosis detection and a ROS Assay Kit (Beyotime) for the detection of reactive oxygen species (ROS) levels according to the manufacturer's instructions. Apoptosis and ROS levels were detected using flow cytometry (FACScan; BD Biosciences), and the results were analyzed using FlowJo software (https://www.flowjo.com/solutions/flowjo).

Cytoprotection Assay

The mRTECs (1×10^5 cells/well) were seeded in 24-well plates with 2.5 μg/mL of Cis for 6 h. The control and Cis groups were switched to normal medium. For the other two groups, after mRTECs were treated with 2.5 μg/mL Cis for 6 h, the NP-labeled or unlabeled MSCs were co-cultured in the 24-well Transwell plates for 24 h. CCK8 assays were used to evaluate the growth inhibition of mRTECs.

Measurement of Lactate Dehydrogenase, l-Glutathione, and Malonaldehyde Levels

After pretreatment with Cis, the supernatants were recovered, and the mRTECs pellets were collected and ground in PBS. The BCA assay kit (Beyotime) was used to determine the total protein concentration in cultured cells or kidney tissues. ELISA kits (Shanghai Enzyme-linked Biotechnology Co. Ltd., Shanghai, China) were used to determine lactate dehydrogenase (LDH), l-glutathione (GSH), and malonaldehyde (MDA) levels. All the procedures were carried out in accordance with the manufacturer's protocol.

Animal Studies Using Mouse Model

Six- to eight-week-old C57BL/6 male mice were obtained from Beijing Sipeifu Experimental Animal Technology Co., Ltd. (Beijing, China) and housed in standard conditions with 12 h-dark/light cycle and ad libitum access to water and food. All experiments were performed in compliance with the regulations and guidelines of the "Guidelines for the Ethical Review of Laboratory Animal Welfare (GB/T 35892–2018)." The Jilin University Animal Welfare and Research Ethics Committee approved all the protocols and animal studies.

To induce AKI, Cis (18 mg/kg) was injected intraperitoneally into mice via a single dose. After 24 h, mice were randomly divided into four groups and received intravenous tail injections as follows: group 1, PBS (PBS 100 μL); group 2, MSC (5×10^5 cells/mouse); group 3, MSCs labeled with NPs (MSC-NP) (5×10^5 cells/mouse); and group 4, magnetically-targeted MSC treatment group (MSC-NP-MAG) (5×10^5 cells/mouse). Each group consisted of 15 mice.

In group 4, after injection of NP-labeled MSCs, a magnet (1.2 T) was placed immediately below the renal region for 20 min. Control animals did not receive Cis injections. On day 7 post-Cis injection, the mice were euthanized, and blood, urine, and kidney samples were harvested for subsequent experiments.

To locate MSCs in the AKI kidney, mice in groups 2 (n=3), 3 (n=3), and 4 (n=3) were administered an intravenous injection of Cy5.5 (Yuanye Biotechnology Co., Ltd, Shanghai, China)-labeled MSCs (with or without NP labeling, 5×10^5 cells/mouse). After 24 h, the kidneys were removed from the mice and observed using a small animal imaging system (Guangzhou Guangyi Biotechnology Co. Ltd., Guangzhou, China).

Biochemical Analysis

Blood urea nitrogen (BUN) and plasma creatinine (Cr) levels were measured using biochemical detection kits (Nanjing Jiancheng Bioengineering Institute, Nanjing, China), according to the manufacturers' protocols.

Measurement of Serum Cytokine Levels

Levels of inflammatory cytokines in serum samples were measured using the Luminex multiplex assay according to the manufacturer's protocol as previously described.[36] Tumor necrosis factor (TNF)-α, interleukin (IL)-1β, IL-2, IL-4, IL-5, IL-10, IL-12, and interferon (IFN)-γ were tested. The results were analyzed using Milliplex Array V5.1 software (Luminex Corporation, Austin, TX, USA).

Histology

Tissue samples were sectioned into 3-μm slices and stained with hematoxylin and eosin (HE) or periodic acid–Schiff (PAS) using standard methods. The stained slices were photographed under a microscope (M8; PreciPoint, Freising, Germany). Histological assessment was performed in a blinded manner.

Immunohistochemistry

Kidney sections were deparaffinized and hydrated, and antigen retrieval sections were then blocked and labeled overnight at 4 °C with primary antibodies, including anti-8-hydroxy-2′-deoxyguanosine (8-OHdG) (Santa Cruz Biotechnology, Dallas, TX, USA), CD3, CD11b, CD68, Ki67, KIM-1, and TIMP-1 (Proteintech, Wuhan, China). Next, the sections were incubated with diluted secondary antibody for 1 h and then treated with 3, 3-diaminobenzidine (DAB) (Vector Laboratories, Burlingame, CA, USA). Slides were photographed using a microscope (M8; PreciPoint). mRTECs in different groups were fixed in 4% paraformaldehyde for 15 min in vitro. Next, cells were incubated with a primary antibody against 8-OHdG overnight at 4 °C. The cells were then incubated with a secondary antibody for 30 min at room temperature. The cells were visualized using a DAB substrate and counterstained with hematoxylin. The cell sections were evaluated using a light microscope (CKX 41; Olympus). Immunohistochemical evaluation was performed in a blinded manner.

Terminal Deoxynucleotidyl Transferase-Mediated dUTP-Biotin Nick-End Labeling Staining

The tissue slices were deparaffinized and dehydrated. Renal tubular cell apoptosis was measured using a Terminal deoxynucleotidyl transferase-mediated dUTP-biotin nick-end labeling (TUNEL) detection kit (Servicebio, Wuhan, China) according to the manufacturer's guidelines. Renal sections were quantitatively analyzed by counting TUNEL-positive cells and compared among different groups.

Statistical Analysis

All values are presented as mean ± standard deviation. Statistical analysis of the data was conducted using SPSS software (v.22.0; IBM Corp., Chicago, IL, USA). The data were assessed for normality (eg, using Shapiro–Wilk test), and variance homogeneity was tested before performing analysis of variance (ANOVA) and *t*-tests. A *t*-test was used for comparison between the two groups. For multiple comparisons among three or more groups, a one-way ANOVA was performed, followed by the Bonferroni test. $P < 0.05$ was considered to be statistically significant for all analyses. All experiments were performed in triplicate.

Results and Discussion

The shape and size of the Fe_3O_4@PDA NPs are consistent with those in our previous research.[36] Internalization of Fe_3O_4@PDA NPs by PL-MSCs was confirmed by Prussian blue staining and TEM analysis. Prussian blue staining showed that MSCs in the unlabeled control group were not positive, whereas for the cells incubated with the NPs (50 μg/mL or 100 μg/mL), almost all MSCs were positive for Prussian blue staining (Figure 1A). It showed that the Prussian blue staining was stronger in the 50 μg/mL group than in the higher dose-groups of 100, 150, and 200 μg/mL. Higher concentrations of NPs can cause aggregation, reduce Brownian motion, and thus prevent cellular uptake of NP aggregates.[37] TEM analysis showed that NPs were localized within endosome-like structures in the cytoplasm of PL-MSCs (Figure 1B).

The utility of NP-labeled cells for stem cell therapy largely depends on the level of cytotoxicity induced by NPs. CCK8 analysis revealed no significant differences in viability between MSC-NPs and PL-MSCs without NPs when the NP concentration in the incubation media was below 100 μg/mL (Figure 1C). However, NPs at the concentration of 150 or 200 μg/mL exhibited cytotoxicity ($P<0.01$). This was in agreement with the results of previous studies showing low cytotoxic effects of Fe_3O_4 NPs.[38,39] According to the CCK8 assay, cell proliferation was not significantly affected at NP concentrations of 25 and 50 μg/mL (Figure 1D). Taken together, our data indicated that low concentrations of NPs were not toxic to MSCs. Subsequent experiments were conducted using NPs with a concentration of 50 μg/mL.

To determine the effect of NP on the basic characteristics of MSCs, we evaluated the expression of surface markers and differentiation ability on labeled MSCs. Comparison of the expression of mesenchymal markers in unlabeled and labeled MSCs showed that NPs did not affect the immunophenotype of the MSCs (Figure S1). Additionally, adipogenic or osteogenic induction culture medium was added to labeled and unlabeled PL-MSCs to induce their differentiation into either adipogenic or osteogenic lineages. Regardless of whether NPs were incorporated, the cells differentiated into the lineages in a similar manner (Figure S1). Taken together, our data indicate that NPs are nontoxic to PL-MSCs and do not compromise their stem cell characteristics. Several studies have explored the varying effects of different types of magnetic particles on MSCs viability, proliferation, differentiation, and gene expression.[40] In most studies, magnetic labeling did not affect MSC function.[41,42]

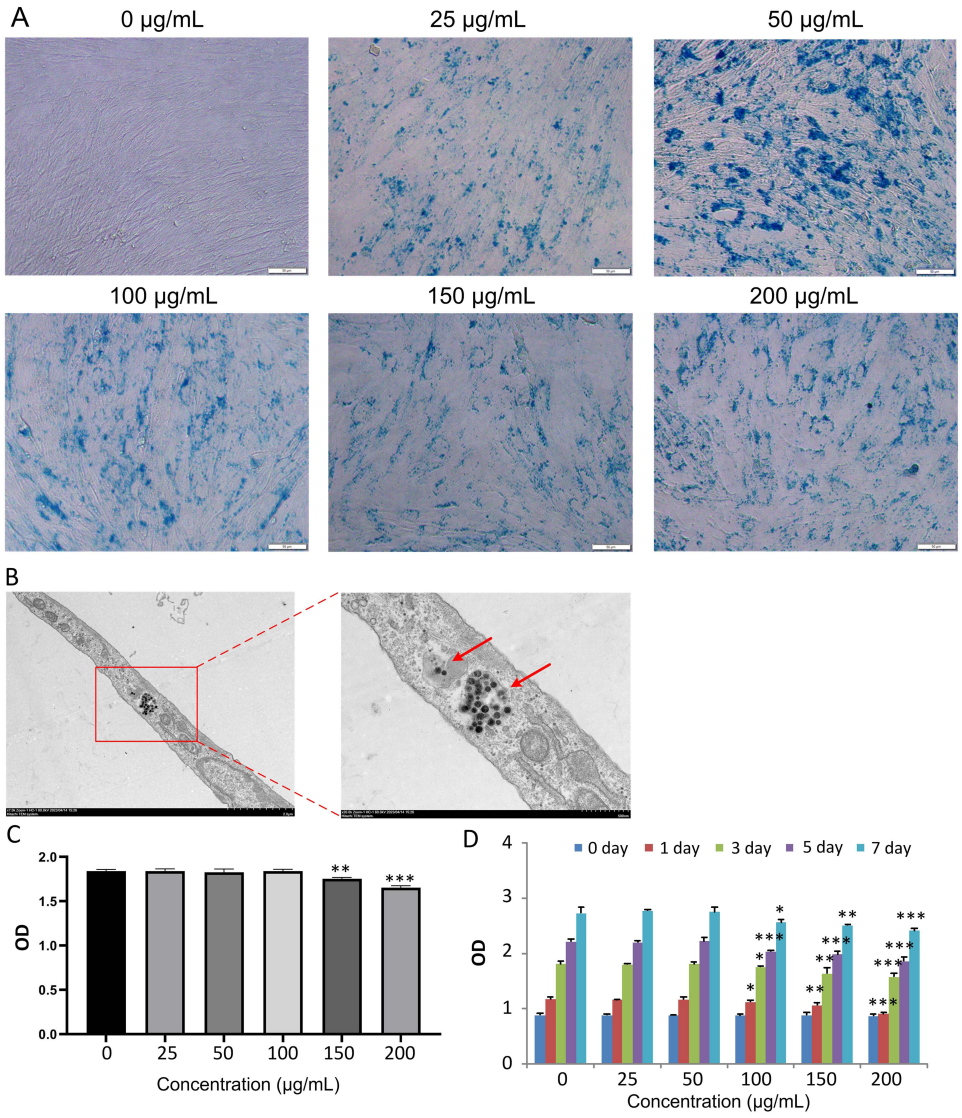

Figure 1 Effects of Fe_3O_4@PDA NP-labeling on the cytotoxicity and proliferation of PL-MSCs. (**A**) Prussian blue staining of Fe_3O_4@PDA NP-labeled PL-MSCs. Scale bar, 50 μm. (**B**) TEM image showing the entry of NPs into cells (arrows). (**C**) Fe_3O_4@PDA NPs cytotoxicity at different concentrations investigated using the CCK8 assay (n=4), revealing that these NPs are not toxic to the cells at doses up to 100 μg/mL. (**D**) Cell proliferation on CCK8 after Fe_3O_4@PDA NP labeling (n=5). Data are expressed as the mean ± SD. *P*-values < 0.05 indicate statistical significance, denoted as **P* < 0.05, ***P* < 0.01, or ****P* < 0.001.

Abbreviations: Fe_3O_4@PDA, Fe_3O_4 nanoparticles coated with polydopamine; PL-MSCs, placental-derived mesenchymal stem cells; TEM, transmission electron microscopy; CCK8, cell-counting kit 8; NP, nanoparticle; SD, standard deviation.

We then evaluated the protective effect of NP-labeled MSCs against Cis-induced mRTEC injury. Analysis of mRTECs exposed to Cis for 6 h with or without MSCs or MSC-NP showed that, compared with the Cis group, the mRTECs co-cultured with MSCs or MSC-NP showed a higher survival rate after Cis treatment (P<0.001; Figure 2A), with an approximate 2.3-fold change. Cis-induced mRTEC injury caused significant cell injury as indicated by LDH release. MSCs (0.53±0.01 pg/mL) and MSC-NP (0.52±0.01 pg/mL) significantly reversed Cis-induced LDH release (1.12±0.01 pg/mL; P<0.001; Figure 2B). Flow cytometry analysis revealed that the apoptosis rate of MSCs (13.83 ±1.58%) or MSC-NP (13.34±0.24%) co-cultured cells was lower after Cis treatment than that in the Cis group (40.87 ±2.98%; P<0.001; Figure 2C and D). Moreover, no significant differences in the optical density values and apoptosis rates of mRTEC were observed between the MSCs and MSC-NP co-culture systems. These results suggest that MSCs and MSC-NPs may have a protective effect on renal tubular cells through paracrine mechanisms, which was consistent

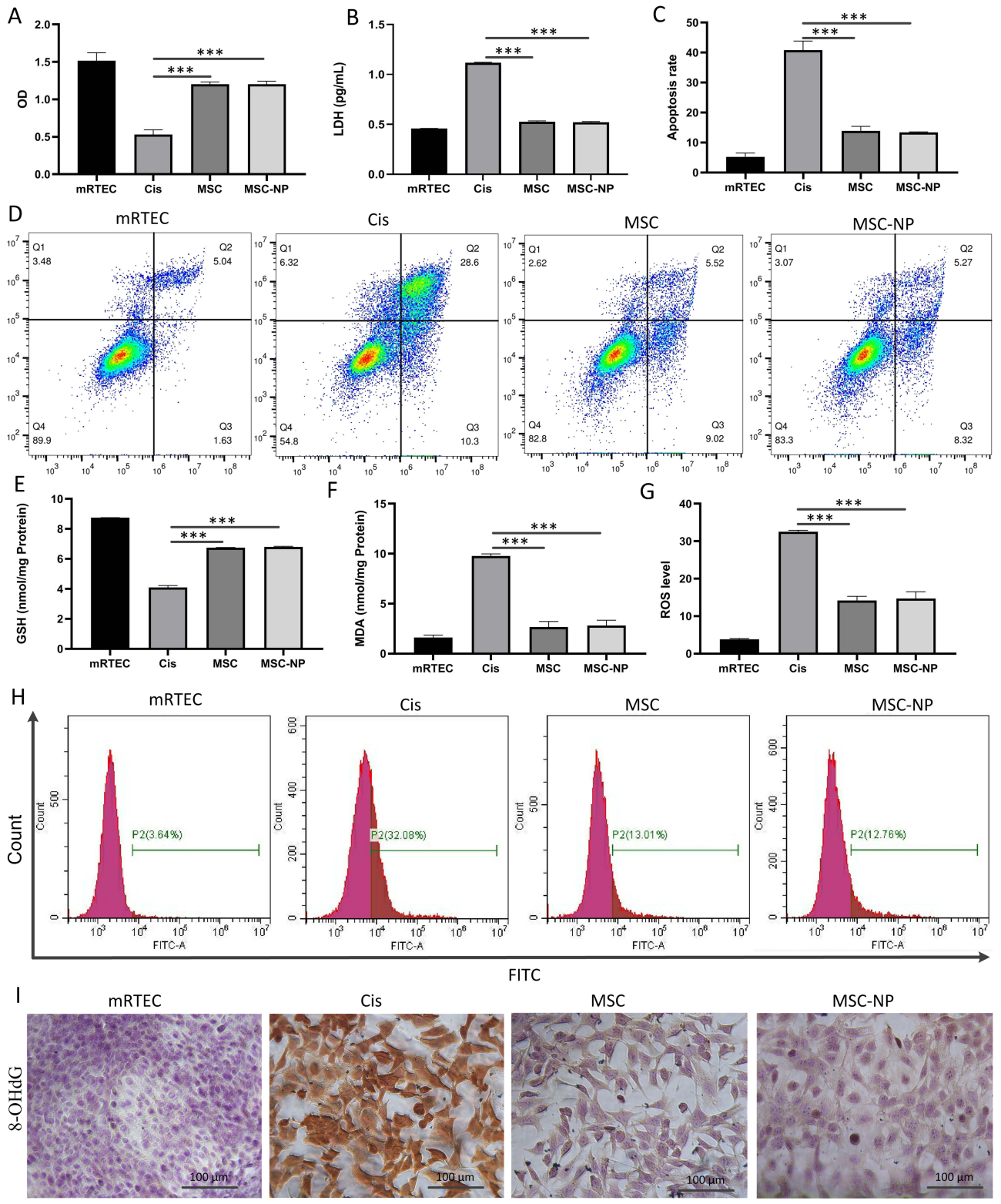

Figure 2 NP-labeled MSCs protect against Cis-induced mRTEC injury in vitro. (**A**) The cell viability of mRTECs co-cultured with MSCs or NP-labeled MSCs using the CCK8 assay (n=4). (**B**) LDH release of mRTECs co-cultured with MSCs or NP-labeled MSCs (n=3). (**C**) The apoptosis rate of mRTECs co-cultured with MSCs or NP-labeled MSCs (n=3). (**D**) The percentage of apoptotic cells in different groups determined by flow cytometry analysis. (**E**) GSH (n=3) and (**F**) MDA (n=3) levels examination in cell homogenates. GSH levels decrease and MDA levels increase in the Cis group; this is reversed in MSC and NP-labeled MSC groups. (**G**) ROS level in mRTECs co-cultured with MSCs or NP-labeled MSCs (n=3). (**H**) Representative images of the flow cytometry data of the ROS assay in mRTECs. (**I**) Immunohistochemistry was used to detect the oxidative stress marker 8-OHdG. Scale bar, 100 μm. Data are expressed as the mean ± SD. *P*-values < 0.05 indicate statistical significance, denoted as ***$P < 0.001$.

Abbreviations: NP, nanoparticle; MSCs, mesenchymal stem cells; mRTECs, conditionally immortalized mice renal tubular endothelial cells; CCK8, cell-counting kit 8; LDH, lactate dehydrogenase; GSH, glutathione; MDA, malondialdehyde; ROS, reactive oxygen species; 8-OHdG, 8-hydroxy-2' -deoxyguanosine; SD, standard deviation.

https://doi.org/10.2147/IJN.S528752

with previous findings.[43,44] The above results indicated that co-culture with MSCs or MSC-NPs enhanced the cellular and anti-apoptotic activity of mRTECs.

Cis-induced oxidative stress in mRTECs is considered the main cause of AKI. Oxidative stress causes lipid peroxidation, resulting in the formation of the toxic metabolite, MDA, and the induction of DNA oxidative damage.[45,46] In this study, MSCs and MSC-NP played antioxidant roles. GSH levels were reduced, and MDA levels were remarkably enhanced in the Cis-treated group compared to those in the normal group. When comparing the MSC- and MSC-NP-treated groups with the PBS and Cis groups, GSH levels increased (4.09±0.12 vs 6.75±0.09 nmol/mg or 4.09±0.12 vs 6.79±0.46 nmol/mg; $P<0.001$), whereas the MDA levels decreased (9.77±0.05 vs 2.67±0.14 nmol/mg or 9.77±0.05 vs 2.81±0.14 nmol/mg; $P<0.001$; Figure 2E and F) in the former groups. The toxicity induced by Cis is closely related to ROS production, which leads to oxidative stress.[47] Flow cytometry results showed that total ROS levels (32.51±0.4%) were elevated in mRTECs after Cis stimulation; however, they are dramatically decreased by MSC (14.18±1.09%) or MSC-NP treatment (14.71±1.82%; $P<0.001$; Figure 2G and H). In vitro experiments showed that 8-OHdG was notably increased in the Cis-treated group, whereas it was decreased in the MSC- and MSC-NP-treated groups (Figure 2I). 8-OHdG expression was similar in the MSC- and MSC-NP-treated groups. These results further support the involvement of oxidative stress in Cis-induced nephrotoxicity,[48] supporting the use of MSC-NPs for the clinical treatment of Cis-induced AKI.

After inducing AKI with Cis for 24 h, mice were treated with MSCs. Compared with the normal group, the PBS group showed a reduction in the survival of mice with AKI on day 7 (100% vs 53%; $P<0.001$; Figure 3A). Compared with the PBS group, all three MSC treatment groups showed improved survival ($P<0.001$). However, the survival rate of mice in the magnetically-targeted MSC treatment group was improved compared to that in the MSC treatment group (94% vs 80%; $P<0.001$) or MSC-NP treatment group (94% vs 80%; $P<0.001$). A similar trend was observed regarding kidney weight following Cis administration. Compared with that in the normal group, the kidney weight of mice in the PBS group was significantly reduced (20.87±1 vs 13.9±0.2 g; $P<0.001$). Compared with the PBS group, the three MSC treatment groups partially prevented the reduction in kidney weight, and the magnetically-targeted MSC treatment group showed the greatest prevention in kidney weight reduction (13.9±0.2 vs 19.83±1 g; $P<0.001$; Figure 3B). However, compared to the MSC treatment group, mice treated with magnetically-targeted MSC showed improved body weight (19.83±1 vs17.4±0.7 g; $P<0.001$). These trends were also observed in the analysis of serum biochemical indices.

To investigate whether MSC treatment contributes to the recovery of kidney function, BUN and Cr levels were measured. The kidney function of AKI mice was remarkably worsened, indicated by the increase in BUN (16.26±2.2 vs 133.76 ±6.04 μmol/L) and Cr (6.21±0.4 vs 66.06± 8.47 μmol/L) levels (Figure 3C and D). Compared with the PBS group, the three MSC treatment groups showed remarkably reduced levels of BUN and Cr, whereas the magnetically-targeted MSC treatment group showed a more significant effect (BUN: 133.76±6.04 vs 29.07±1.48 μmol/L; $P<0.001$; Cr: 77.77± 0.74 vs 16.39±0.58 μmol/L; $P<0.001$). Meanwhile, the BUN and Cr levels in the magnetically-targeted therapy group were significantly lower than those in the MSC treatment group (BUN: 29.07±1.48 vs 51.22±1.25 μmol/L; $P<0.001$; Cr: 16.39 ±0.58 vs 34.12± 3.28 μmol/L; $P<0.001$) and MSC-NP treatment group (BUN: 29.07±1.48 vs 51.12±1.04 μmol/L; $P<0.001$; Cr: 16.39±0.58 vs 35.87± 3.29 μmol/L; $P<0.001$). GSH levels were decreased (2.29±0.12 vs 4.41±0.18 nmol/mg; $P<0.001$), and MDA levels were significantly increased (12.39±0.62 vs 5.21±0.05 nmol/mg; $P<0.001$) in the Cis-treated group compared with those in the normal group. Reduction in the total renal GSH level was clearly inhibited in the magnetically-targeted MSC treatment group (3.63±0.09 vs 2.29±0.12 nmol/mg; $P<0.001$; Figure 3E). The increase in renal MDA levels was also significantly inhibited in the magnetically-targeted MSC treatment group (6.77±0.11 vs 12.39±0.62 nmol/mg; $P<0.05$; Figure 3F). Additionally, the magnetically-targeted MSC treatment group had a stronger effect in reversing the decrease in GSH levels and the increase in MDA levels than the MSC treatment group (GSH: 3.63±0.09 vs 3.34±0.1 nmol/mg; $P<0.05$; MDA: 6.76±0.11 vs 7.98±0.16 nmol/mg; $P<0.001$) and MSC-NP treatment group (GSH: 3.63±0.09 vs 3.33±0.1 nmol/mg; $P<0.05$; MDA: 6.76±0.11 vs 8.06±0.11 nmol/mg; $P<0.001$). Oxidative stress leads to the production of the harmful lipid product, MDA.[45] Meanwhile, the activity of the antioxidant defense enzymes decrease,[49] leading to cell damage. These changes cause a change in oxidative stress markers: decreased levels of the antioxidant enzyme, GSH, and increased expression of MDA. In this study, we observed that magnetically-targeted MSCs exerted significant antioxidant effects.

Studies have reported that labeled cells (PKH26, DiI, and DID) were mostly detected in the lungs and much less in the liver and kidneys.[36,44,50] The number and survival of engrafted MSCs in the lesion directly affect the repair outcomes

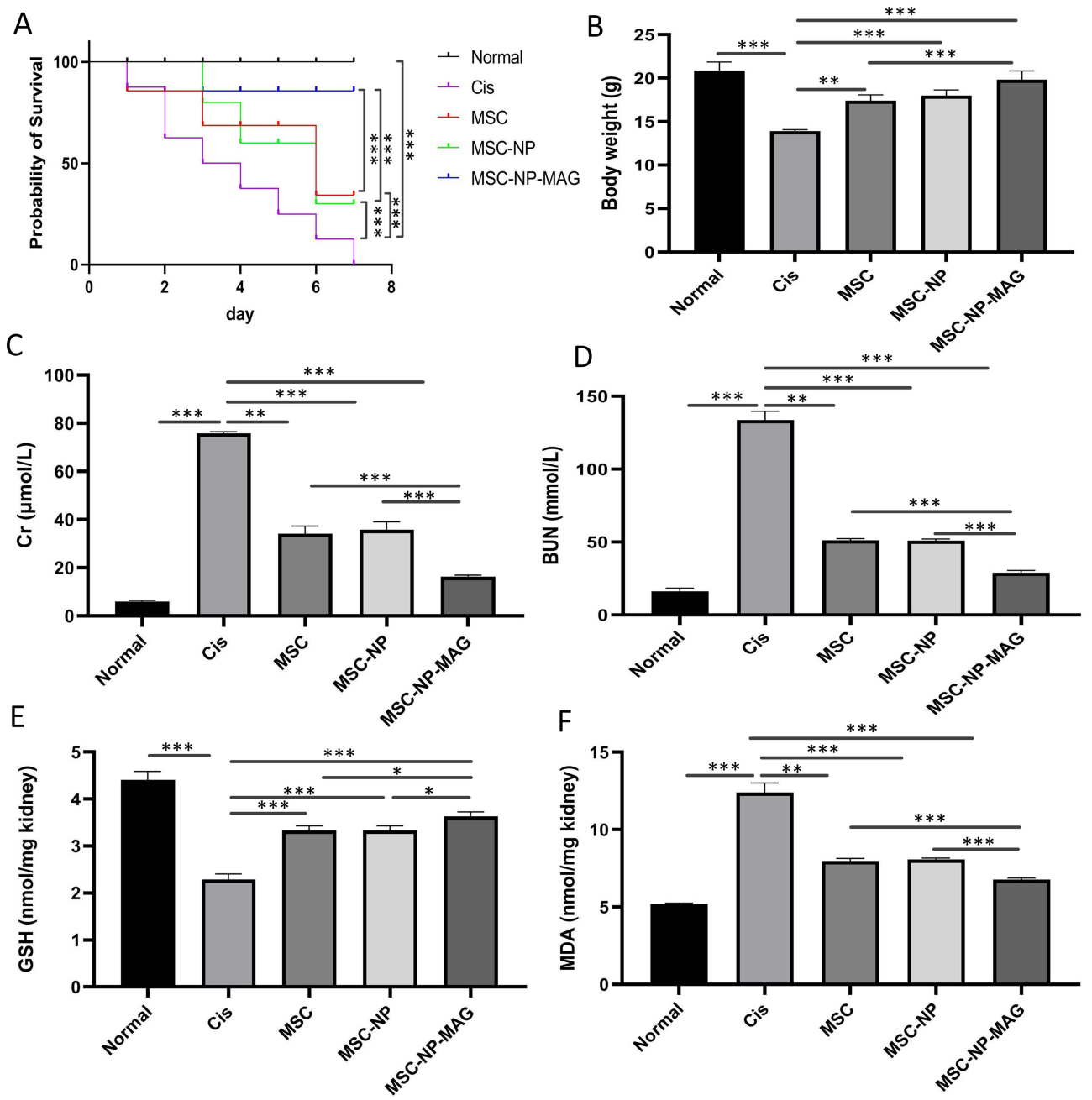

Figure 3 Magnetically-targeted MSC treatment reduces the clinical manifestations of AKI. (**A**) The survival rate of mice in each experimental group. (**B**) Weight changes of mice during treatment (n=3). Cr (**C**) and BUN (**D**) levels in mice (n=3 for each group). GSH (**E**) and MDA (**F**) levels examined in kidney tissue homogenates with the respective detection kits (n=3 for each group). Data are expressed as the mean ± SD. *P*-values < 0.05 indicate statistical significance, denoted as **P* < 0.05, ***P* < 0.01 and ****P* < 0.001.
Abbreviations: MSC, mesenchymal stem cell; AKI, acute kidney injury; Cr, creatinine; BUN, blood urea nitrogen; GSH, glutathione; MDA, malondialdehyde; SD, standard deviation.

of MSC transplantation strategies. The approach for targeting MSCs involves magnetic guidance, wherein cells labeled with magnetic NPs are directed toward the target organ using an external magnetic field.

To confirm whether the magnetically-targeted MSCs migrated to the kidneys, fluorescence imaging was performed. For in vivo fluorescence imaging, MSCs were labeled with Cy5.5 before injection. Fluorescence imaging 24 h after injection showed that in the MSC or MSC-NP group, a small number of MSCs accumulated in the kidney, whereas in the magnetically-targeted MSC group, a large number of cells targeted the kidney (Figure 4A). These findings indicate that more MSCs homed to the injured kidneys in the magnetic group than in the other two non-magnetic groups. The

https://doi.org/10.2147/IJN.S528752

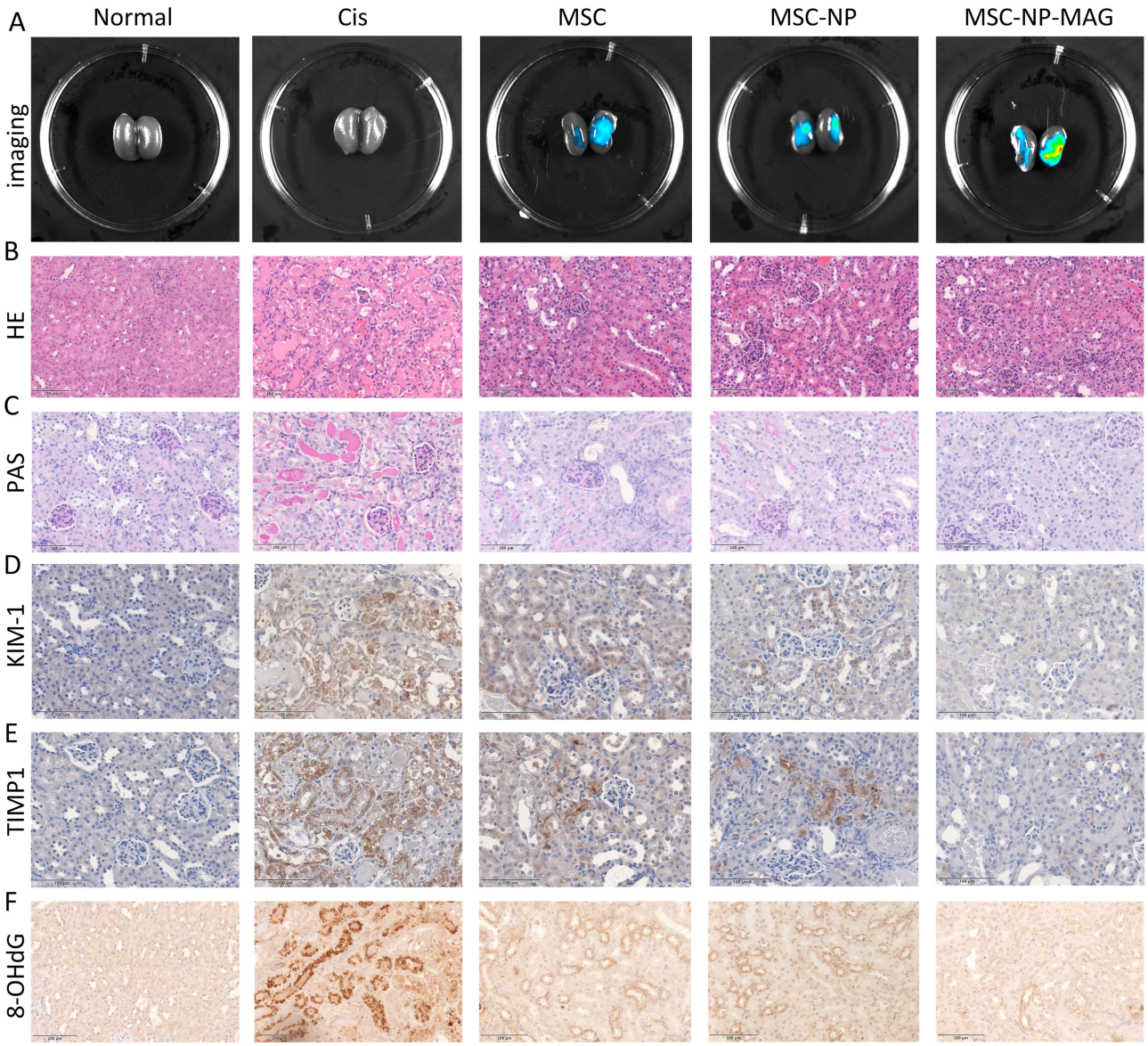

Figure 4 Magnetically-targeted MSC treatment reduces structural renal injuries in AKI mice models. (**A**) Live animal images of injured pancreas after injection of NP-labeled or unlabeled MSC with or without magnetic field. (**B**) Representative histology of kidney tissues by HE staining. Scale bar, 100 μm. (**C**) Representative images of PAS staining. Scale bar, 100 μm. (**D** and **E**) Immunohistochemical staining showing expression of injury markers KIM-1 and TIMP-1. Scale bar, 100 μm. (**F**) Immunohistochemistry was used to detect the oxidative stress marker 8-OHdG. Scale bar,100 μm.

Abbreviations: MSC, mesenchymal stem cell; AKI, acute kidney injury; NP, nanoparticle; HE, hematoxylin and eosin; PAS, periodic acid Schiff; 8-OHdG, 8-hydroxy-2'-deoxyguanosine.

magnetically-targeted MSC group improved therapeutic efficacy by increasing the delivery of therapeutic cargo to the target site and avoiding isolation of cell therapy.

HE staining of kidney tissue revealed that Cis induced significant kidney injury, such as extensive swelling, vacuolar degeneration, and detachment of epithelial cells, whereas kidney injury was largely weakened in mice treated with MSCs or MSC-NPs (Figure 4B). PAS staining showed severe renal histological abnormalities in mice, including tubular cell detachment, tubular cell death, and cast formation, whereas kidney damage was significantly reduced in mice treated with MSC or MSC-NPs. The kidneys from magnetically-targeting MSC-treated mice showed a nearly normal morphology (Figure 4C). However, mice in the magnetically-targeted MSC group showed less histological evidence of kidney injury than those in the MSC or MSC-NP groups. To test the protective features of MSC or MSC-NPs on renal tubules, KIM-1 and TIMP-1 (tubule injury markers[51,52]) were evaluated. Immunohistochemistry staining revealed that the normal group did not express KIM-1 and TIMP1, but Cis-induced AKI remarkably upregulated both markers (Figure 4D and E). The

MSC and MSC-NP groups showed partially reduced expression of KIM-1 and TIMP1. Moreover, the magnetically-targeted MSC group almost completely eliminated their presence. Similar to the results of the in vitro experiments, 8-OHdG, a key biomarker widely used for studying oxidative injury-related diseases,[53] was notably increased in the Cis-treated group in vivo but declined significantly in the MSC- or MSC-NP-treated groups (Figure 4F). Among the three MSC treatment groups, the magnetically-targeted MSC experimental group showed the lowest 8-OHdG expression. Overall, these data indicate that MSCs and MSC-NPs can alleviate Cis-induced renal injury and oxidative stress in mice; however, magnetically-targeted MSCs are more effective.

Inflammation plays an important role in Cis nephrotoxicity.[54,55] T-cells, natural killer (NK) cells, and macrophages play a critical role in mediating injury repair and renal function recovery in AKI.[56] The changes in immune cell populations are summarized in Figure 5A. The number of CD68-positive macrophages and CD3-positive T cells in Cis-treated mice (no MSCs) was significantly higher. After treatment with MSCs alone or MSC-NPs, the expression of CD68 and CD3 decreased.

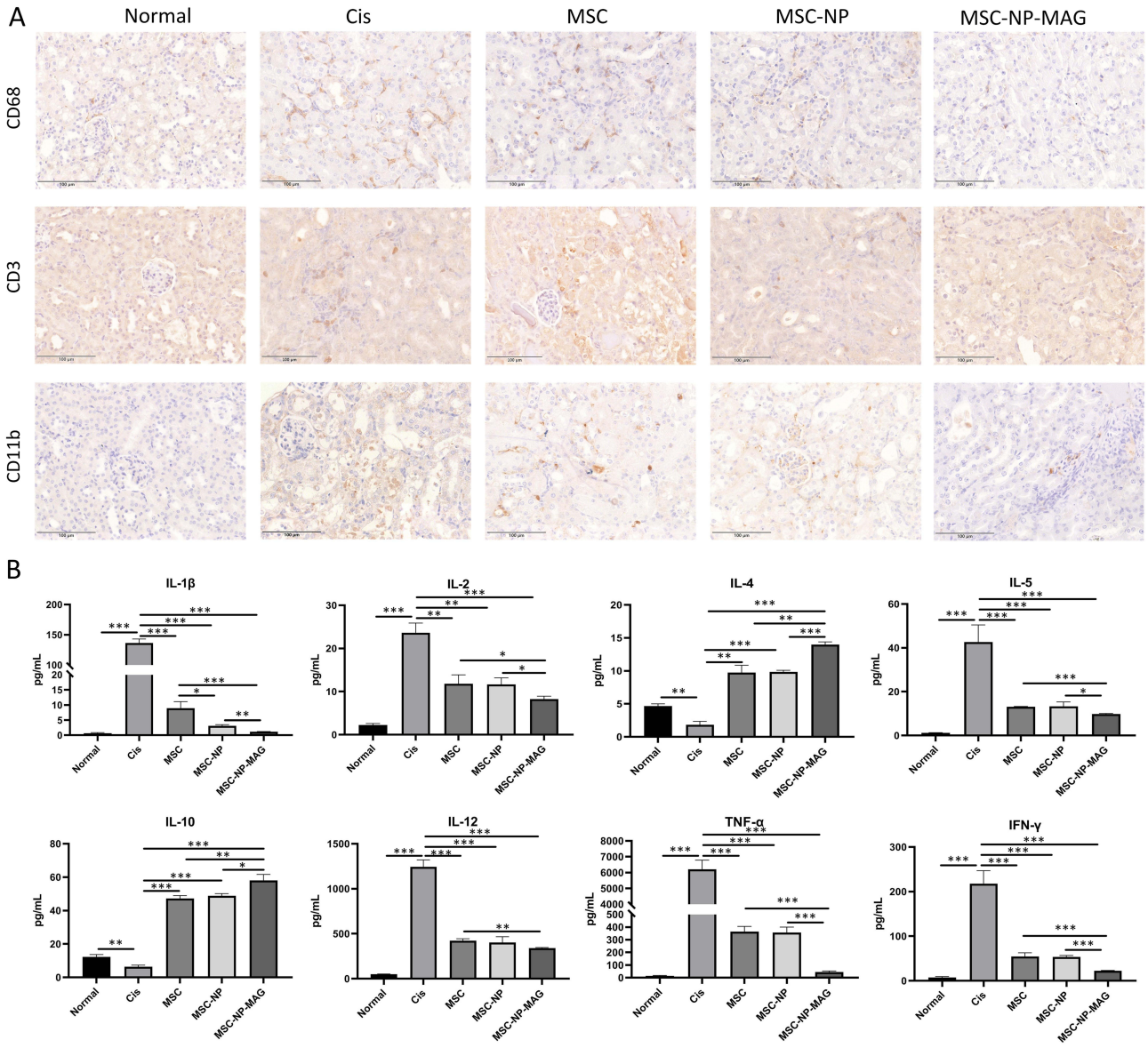

Figure 5 Enhanced anti-inflammatory efficacy of magnetically-targeted MSCs in AKI mice. (**A**) Representative immunostaining images of CD68+ macrophages, CD3+ T cells, or CD11b+ NKs in the tubulointerstitium. Scale bar, 100 μm. (**B**) Inflammatory cytokine concentrations in the blood serum. Each group has three mice. Data are expressed as the mean ± SD. *P*-values < 0.05 indicate statistical significance, denoted as **P* < 0.05, ***P* < 0.01, or ****P* < 0.001.

Abbreviations: MSC, mesenchymal stem cell; AKI, acute kidney injury; NKs, natural killer cells; SD, standard deviation.

https://doi.org/10.2147/IJN.S528752

In addition, interstitial infiltration of inflammatory cells in the kidney was markedly inhibited by the combination of magnetically-targeted MSC. CD11b expression by NK cells was significantly reduced by MSCs alone, and MSC-NP treatment was further reduced by the combination of magnetically-targeted MSCs. One possible repair mechanism involves MSCs combating inflammation by reducing multiple inflammatory cytokines or secreting several anti-inflammatory factors.[57] We evaluated the serum levels of various cytokines to investigate the effects of the three MSC groups on systemic inflammation and observed that the levels of IL-1β, IL-2, IL-5, IL-12, IFN-γ, and TNF-α in mouse serum of the magnetically-targeted MSC-treated group were lower than those in the MSC or MSC-NP-treated groups ($P<0.05$, Figure 5B). These data suggest that the anti-inflammatory efficacy of the combination of magnetically-targeted MSCs was significantly higher than that of MSCs alone or that of MSC-NP treatment. Collectively, these results suggest that the magnetically-targeted MSCs can alleviate murine AKI and mitigate proximal tubular injury. The anti-inflammatory activity of MSCs is believed to be the major mechanism by which they protect against renal damage.[58] In the present study, the magnetically-targeted MSCs may reduce local inflammatory responses by increasing the number of MSCs retained at the site of injury, enhancing paracrine effects and inhibiting inflammatory cell infiltration and cytokine secretion.

A characteristic pathological manifestation of AKI consists of necrosis and loss of renal tubular epithelial cells.[59] Modulation of cell proliferation and apoptosis may be another mechanism by which MSCs exert their therapeutic effects.[60] Compared with the normal group, the AKI group had dramatically reduced Ki67+ cells in the kidney (Figure 6A). A marked increase in Ki67+ cells in the MSC-treated groups was observed compared with that in the PBS control group (4.33±1.04% vs 16.4±1.28%; $P<0.001$). Compared to those in the magnetically-targeted MSCs group, the Ki67+ cells in the MSC group (24±1.73% vs 16.4 ±1.28%; $P<0.01$) and MSC-NP group showed significant reduction (24±1.73% vs 16.17±1.26%; $P<0.01$; Figure 6C). This result indicates that magnetically-targeted MSCs can enable a larger proportion of MSCs to reach the site of injury, providing greater and more sustained release of mediators, thereby achieving the ability to repair injury tissue cell proliferation.

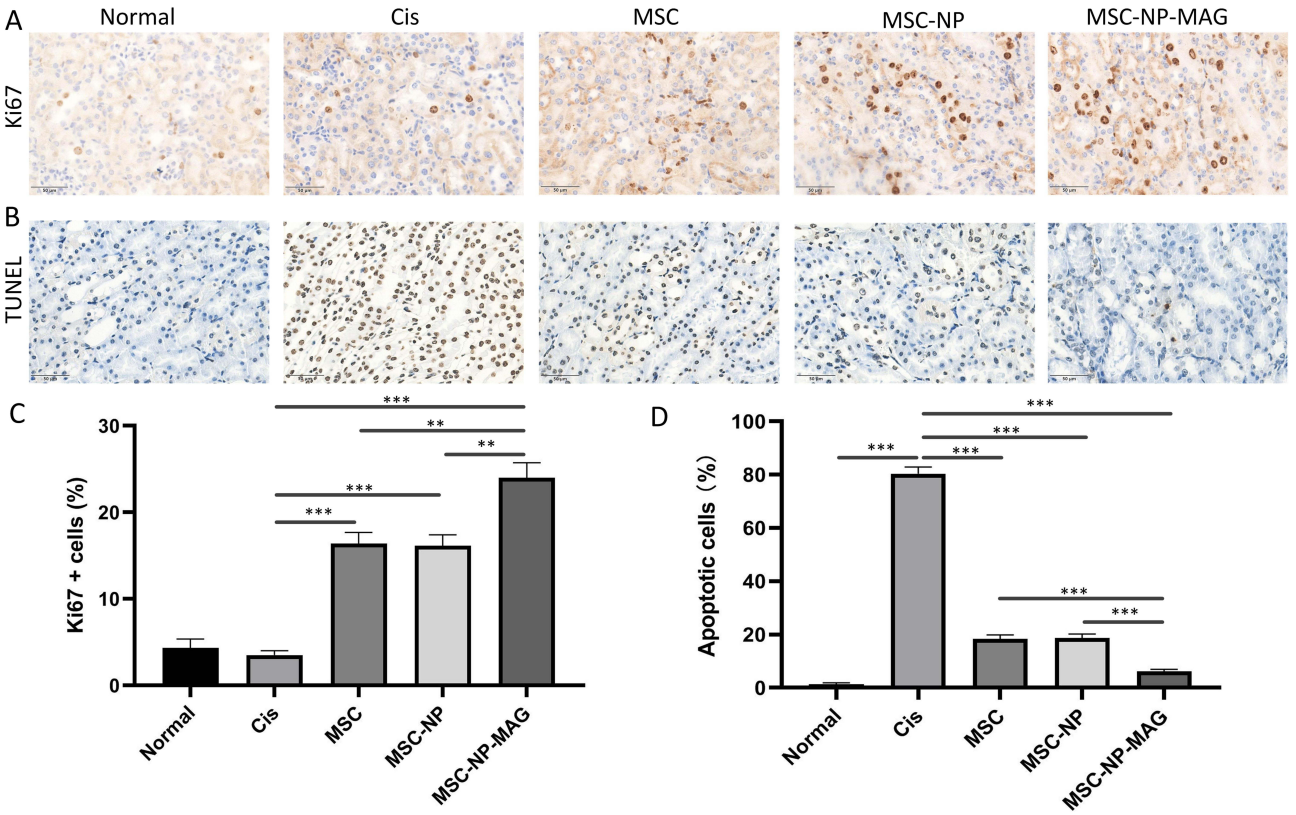

Figure 6 Magnetically-targeted MSCs promote proliferation and inhibit apoptosis. Immunohistochemical staining of Ki67 (**A**) and TUNEL (**B**) staining of kidney tissues in each group. Scale bar, 100 μm. (**C**) Histograms showing the percentage of Ki67 (+) cells (n=3). (**D**) Histograms showing the percentage of TUNEL (+) cells (n=3). Each column presents data as the mean ± SD. *P*-values < 0.05 indicate statistical significance, denoted as $^{**}P < 0.01$, or $^{***}P < 0.001$.

Abbreviations: MSCs, mesenchymal stem cell; TUNEL, terminal deoxynucleotidyl transferase-mediated dUTP-biotin nick-end labeling; SD, standard deviation.

Accumulating evidence has shown that apoptosis plays a crucial role in Cis-induced nephrotoxicity.[61–63] TUNEL staining revealed that Cis significantly increased apoptosis compared with that in the normal group, but this effect was significantly decreased in all MSC-treated groups compared with that in the PBS group (Figure 6B). The apoptosis rate was lower in the magnetically-targeted treatment group than in the MSC (6.16±0.62% vs 18.33±1.24%; $P<0.001$) and MSC-NP treatment groups (6.16±0.62% vs 18.67±1.24%; $P<0.001$; Figure 6D), further corroborating the above findings. The magnetically-targeted MSCs significantly inhibited Cis-induced apoptosis in AKI compared with MSCs and MSC-NPs. These results indicated that MSC decreased Cis-induced renal apoptosis in mice. Overall, magnetically-targeted MSCs showed more efficient repair ability than MSCs or MSC-NPs in Cis-induced AKI. The magnetically-targeted MSCs successfully restored physiological measures of kidney function, reduced the histological and molecular markers of injury, attenuated local inflammation, and restored proliferative and anti-apoptotic activity, demonstrating its potent regenerative potential. These findings indicate that magnetically-targeted MSCs may represent an effective therapeutic strategy for AKI.

The core mechanism of MSCs for repairing tissue damage involves the release of paracrine or endocrine factors and direct cell–cell interactions.[64] With the application of external magnetic force, magnetized MSCs presented increased expression of integrins and adhesion molecules.[65] These changes may contribute to increased MSC adherence and engraftment to target sites in vivo, which is particularly beneficial to renal applications. Therefore, higher local MSC concentration would arguably result in a greater release of secretory vesicles and soluble factors with immunomodulatory, anti-inflammatory, and potentially repair properties. Although magnetically-targeted MSCs have been shown to enhance the therapeutic efficacy in many experimental models, some safety issues need to be addressed prior to conducting clinical trials using this technique. These concerns include the biocompatibility between MSCs and NPs, the impact of external magnetic field on MSCs, and adverse effects in vivo.

Conclusions

In conclusion, the targeting of labeled MSC into the AKI mouse kidney was achieved with the use of an external magnetic field. We have described a novel and potentially useful treatment approach and provide evidence that the combination of magnetic NP uptake and external magnetic field therapy can increase the number of PL-MSCs at the site of injury, enhance paracrine effects, release more soluble factors with immunomodulatory and anti-inflammatory effects, and improve recovery, outperforming PL-MSC treatment alone. Our research findings indicate that magnetic targeting is a promising and valuable tool that can ameliorate Cis-induced nephrotoxicity by enhancing the aggregation ability of PL-MSC at the site of injury.

Data Sharing Statement

All data generated or analyzed during this study are included in this publication.

Funding

This study was funded by the Department of Science and Technology of Jilin Province (Grant No. YDZJ202401195ZYTS), the Spring Bud Project of the China-Japan Union Hospital of Jilin University (Grant No. 2023CL03), and the Project of Technical Service (No. 2024YX0095).

Disclosure

Ke Wang and Ye Zhao contributed equally to this work and are co-first authors. There are no conflicts of interest to declare.

References

1. Chen Z, Ren X, Ren R, Wang Y, Shang J. The combination of G-CSF and AMD3100 mobilizes bone marrow-derived stem cells to protect against cisplatin-induced acute kidney injury in mice. *Stem Cell Res Ther*. 2021;12(1):209. doi:10.1186/s13287-021-02268-y
2. Ghosh S. Cisplatin: the first metal based anticancer drug. *Bioorg Chem*. 2019;88:102925. doi:10.1016/j.bioorg.2019.102925
3. Yu B, Jin L, Yao X, et al. TRPM2 protects against cisplatin-induced acute kidney injury and mitochondrial dysfunction via modulating autophagy. *Theranostics*. 2023;13(13):4356–4375. doi:10.7150/thno.84655
4. Xiang Y, Ji M, Wu L, et al. Rosmarinic Acid Prevents Cisplatin-Induced Liver and Kidney Injury by Inhibiting Inflammatory Responses and Enhancing Total Antioxidant Capacity, Thereby Activating the Nrf2 Signaling Pathway. *Molecules*. 2022;27(22):7815. doi:10.3390/molecules27227815
5. Deng JS, Jiang WP, Chen CC, et al. Cordyceps cicadae Mycelia Ameliorate Cisplatin-Induced Acute Kidney Injury by Suppressing the TLR4/NF-κB/MAPK and Activating the HO-1/Nrf2 and Sirt-1/AMPK Pathways in Mice. *Oxid Med Cell Longev*. 2020;2020:7912763. doi:10.1155/2020/7912763

6. Yao W, Hu Q, Ma Y, et al. Human adipose-derived mesenchymal stem cells repair cisplatin-induced acute kidney injury through antiapoptotic pathways. *Exp Ther Med*. 2015;10(2):468–476. doi:10.3892/etm.2015.2505
7. Yang L, Wang B, Guo F, et al. FFAR4 improves the senescence of tubular epithelial cells by AMPK/SirT3 signaling in acute kidney injury. *Signal Transduct Target Ther*. 2022;7(1):384. doi:10.1038/s41392-022-01254-x
8. Narcisi R, Koevoet W, van Osch G. Expansion and Chondrogenic Differentiation of Human Bone Marrow-Derived Mesenchymal Stromal Cells. *Methods Mol Biol*. 2021;2221:15–28. doi:10.1007/978-1-0716-0989-7_2
9. Bunnell BA. Adipose Tissue-Derived Mesenchymal Stem Cells. *Cells*. 2021;10(12):34433. doi:10.3390/cells10123433
10. Dapkute D, Steponkiene S, Bulotiene D, Saulite L, Riekstina U, Rotomskis R. Skin-derived mesenchymal stem cells as quantum dot vehicles to tumors. *Int J Nanomed*. 2017;12:8129–8142. doi:10.2147/ijn.S143367
11. Liu H, Wang J, Yue G, Xu J. Placenta-derived mesenchymal stem cells protect against diabetic kidney disease by upregulating autophagy-mediated SIRT1/FOXO1 pathway. *Ren Fail*. 2024;46(1):2303396. doi:10.1080/0886022x.2024.2303396
12. Xu Q, Yan P, Duan XJ, et al. Human umbilical cord-derived mesenchymal stem cells and human cord blood mononuclear cells protect against cisplatin-induced acute kidney injury in rat models. *Exp Ther Med*. 2020;20(6):145. doi:10.3892/etm.2020.9274
13. Kim JH, Park DJ, Yun JC, et al. Human adipose tissue-derived mesenchymal stem cells protect kidneys from cisplatin nephrotoxicity in rats. *Am J Physiol Renal Physiol*. 2012;302(9):F1141–50. doi:10.1152/ajprenal.00060.2011
14. Rabelink TJ, Little MH. Stromal cells in tissue homeostasis: balancing regeneration and fibrosis. *Nat Rev Nephrol*. 2013;9(12):747–753. doi:10.1038/nrneph.2013.152
15. Morigi M, Introna M, Imberti B, et al. Human bone marrow mesenchymal stem cells accelerate recovery of acute renal injury and prolong survival in mice. *Stem Cells*. 2008;26(8):2075–2082. doi:10.1634/stemcells.2007-0795
16. Tang M, Shen L, Tang M, et al. Human mesenchymal stromal cells ameliorate cisplatin-induced acute and chronic kidney injury via TSG-6. *Stem Cells*. 2024;42(9):848–859. doi:10.1093/stmcls/sxae037
17. Lee JM, Jung J, Lee HJ, et al. Comparison of immunomodulatory effects of placenta mesenchymal stem cells with bone marrow and adipose mesenchymal stem cells. *Int Immunopharmacol*. 2012;13(2):219–224. doi:10.1016/j.intimp.2012.03.024
18. Lankford L, Selby T, Becker J, et al. Early gestation chorionic villi-derived stromal cells for fetal tissue engineering. *World J Stem Cells*. 2015;7(1):195–207. doi:10.4252/wjsc.v7.i1.195
19. Shokati A, Naser MA, Ghashghaei A, et al. Good manufacturing practices production of human placental derived mesenchymal stem cells for therapeutic applications: focus on multiple sclerosis. *Mol Biol Rep*. 2024;51(1):460. doi:10.1007/s11033-024-09372-1
20. Levy JA, Marchand M, Iorio L, Cassini W, Zahalsky MP. Determining the Feasibility of Managing Erectile Dysfunction in Humans With Placental-Derived Stem Cells. *J Am Osteopath Assoc*. 2016;116(1):e1–5. doi:10.7556/jaoa.2016.007
21. Payandeh M, Habibi R, Norooznezhad AH, et al. Human placenta-derived mesenchymal stromal cells transfusion in a critically Ill infant diagnosed with Coronavirus Disease 2019 (COVID-19): a case report. *Transfus Apher Sci*. 2022;61(6):103454. doi:10.1016/j.transci.2022.103454
22. Liu J, Lu X, Lou Y, et al. Xenogeneic Transplantation of Human Placenta-Derived Mesenchymal Stem Cells Alleviates Renal Injury and Reduces Inflammation in a Mouse Model of Lupus Nephritis. *Biomed Res Int*. 2019;2019:9370919. doi:10.1155/2019/9370919
23. Qi H, Liu C, Long L, et al. Blood Exosomes Endowed with Magnetic and Targeting Properties for Cancer Therapy. *ACS Nano*. 2016;10(3):3323–3333. doi:10.1021/acsnano.5b06939
24. Vangijzegem T, Stanicki D, Laurent S. Magnetic iron oxide nanoparticles for drug delivery: applications and characteristics. *Expert Opin Drug Deliv*. 2019;16(1):69–78. doi:10.1080/17425247.2019.1554647
25. Bryan MT. Assessing the Challenges of Nanotechnology-Driven Targeted Therapies: development of Magnetically Directed Vectors for Targeted Cancer Therapies and Beyond. *Methods Mol Biol*. 2023;2575:105–123. doi:10.1007/978-1-0716-2716-7_6
26. Wu L, Zhang F, Wei Z, et al. Magnetic delivery of Fe(3)O(4)@polydopamine nanoparticle-loaded natural killer cells suggest a promising anticancer treatment. *Biomater Sci*. 2018;6(10):2714–2725. doi:10.1039/c8bm00588e
27. Lidsky ME, Spritzer CE, Shortell CK. The role of dynamic contrast-enhanced magnetic resonance imaging in the diagnosis and management of patients with vascular malformations. *J Vasc Surg*. 2012;56(3):757–64.e1. doi:10.1016/j.jvs.2012.02.032
28. Chen FH, Zhang LM, Chen QT, Zhang Y, Zhang ZJ. Synthesis of a novel magnetic drug delivery system composed of doxorubicin-conjugated Fe3O4 nanoparticle cores and a PEG-functionalized porous silica shell. *Chem Commun*. 2010;46(45):8633–8635. doi:10.1039/c0cc02577a
29. van Raap MB F, Coral DF, Yu S, Muñoz GA, Sánchez FH, Roig A. Anticipating hyperthermic efficiency of magnetic colloids using a semi-empirical model: a tool to help medical decisions. *Phys Chem Chem Phys*. 2017;19(10):7176–7187. doi:10.1039/c6cp08059f
30. Ge R, Li X, Lin M, et al. Fe3O4@polydopamine Composite Theranostic Superparticles Employing Preassembled Fe3O4 Nanoparticles as the Core. *ACS Appl Mater Interfaces*. 2016;8(35):22942–22952. doi:10.1021/acsami.6b07997
31. Mahmoud EE, Kamei G, Harada Y, et al. Cell Magnetic Targeting System for Repair of Severe Chronic Osteochondral Defect in a Rabbit Model. *Cell Transplant*. 2016;25(6):1073–1083. doi:10.3727/096368915x689613
32. Mai X, Xie Y, Wu Z, et al. Magnetic resonance imaging tracing of superparamagnetic iron oxide nanoparticle-labeled mesenchymal stromal cells for repairing spinal cord injury. *Neural Regen Res*. 2024;2014:10–4103. doi:10.4103/nrr.Nrr-d-24-00431
33. Huang Z, Shen Y, Sun A, et al. Magnetic targeting enhances retrograde cell retention in a rat model of myocardial infarction. *Stem Cell Res Ther*. 2013;4(6):149. doi:10.1186/scrt360
34. Hsu FT, Wei ZH, Hsuan YC, et al. MRI tracking of polyethylene glycol-coated superparamagnetic iron oxide-labelled placenta-derived mesenchymal stem cells toward glioblastoma stem-like cells in a mouse model. *Artif Cells Nanomed Biotechnol*. 2018;46(sup3):S448–s459. doi:10.1080/21691401.2018.1499661
35. Li X, Bai J, Ji X, Li R, Xuan Y, Wang Y. Comprehensive characterization of four different populations of human mesenchymal stem cells as regards their immune properties, proliferation and differentiation. *Int J Mol Med*. 2014;34(3):695–704. doi:10.3892/ijmm.2014.1821
36. Li X, Wei Z, Wu L, et al. Efficacy of Fe(3)O(4)@polydopamine nanoparticle-labeled human umbilical cord Wharton's jelly-derived mesenchymal stem cells in the treatment of streptozotocin-induced diabetes in rats. *Biomater Sci*. 2020;8(19):5362–5375. doi:10.1039/d0bm01076f
37. Pernal S, Wu VM, Uskoković V. Hydroxyapatite as a Vehicle for the Selective Effect of Superparamagnetic Iron Oxide Nanoparticles against Human Glioblastoma Cells. *ACS Appl Mater Interfaces*. 2017;9(45):39283–39302. doi:10.1021/acsami.7b15116

38. Sun J, Wang S, Zhao D, Hun FH, Weng L, Liu H. Cytotoxicity, permeability, and inflammation of metal oxide nanoparticles in human cardiac microvascular endothelial cells: cytotoxicity, permeability, and inflammation of metal oxide nanoparticles. *Cell Biol Toxicol*. 2011;27(5):333–342. doi:10.1007/s10565-011-9191-9
39. Fahmy B, Cormier SA. Copper oxide nanoparticles induce oxidative stress and cytotoxicity in airway epithelial cells. *Toxicol In Vitro*. 2009;23 (7):1365–1371. doi:10.1016/j.tiv.2009.08.005
40. Wang W, Deng Z, Xu X, et al. Functional Nanoparticles and their Interactions with Mesenchymal Stem Cells. *Curr Pharm Des*. 2017;23 (26):3814–3832. doi:10.2174/1381612823666170622110654
41. Landázuri N, Tong S, Suo J, et al. Magnetic targeting of human mesenchymal stem cells with internalized superparamagnetic iron oxide nanoparticles. *Small*. 2013;9(23):4017–4026. doi:10.1002/smll.201300570
42. Yan J, Liu T, Li Y, et al. Effects of magnetically targeted iron oxide@polydopamine-labeled human umbilical cord mesenchymal stem cells in cerebral infarction in mice. *Aging*. 2023;15(4):1130–1142. doi:10.18632/aging.204540
43. Cheng K, Rai P, Plagov A, et al. Transplantation of bone marrow-derived MSCs improves cisplatinum-induced renal injury through paracrine mechanisms. *Exp Mol Pathol*. 2013;94(3):466–473. doi:10.1016/j.yexmp.2013.03.002
44. Yuan L, Wu MJ, Sun HY, et al. VEGF-modified human embryonic mesenchymal stem cell implantation enhances protection against cisplatin-induced acute kidney injury. *Am J Physiol Renal Physiol*. 2011;300(1):F207–18. doi:10.1152/ajprenal.00073.2010
45. Antunes LM, Darin JD, Bianchi MD. Protective effects of vitamin c against cisplatin-induced nephrotoxicity and lipid peroxidation in adult rats: a dose-dependent study. *Pharmacol Res*. 2000;41(4):405–411. doi:10.1006/phrs.1999.0600
46. Allowitz K, Taylor J, Harames K, Yoo J, Baloch O, Ramana KV. Oxidative Stress-mediated Lipid Peroxidation-derived Lipid Aldehydes in the Pathophysiology of Neurodegenerative Diseases. *Curr Neuropharmacol*. 2025;23(6):671–685. doi:10.2174/011570159x342720241014164650
47. Kim HJ, Lee JH, Kim SJ, et al. Roles of NADPH oxidases in cisplatin-induced reactive oxygen species generation and ototoxicity. *J Neurosci*. 2010;30(11):3933–3946. doi:10.1523/jneurosci.6054-09.2010
48. Pei Z, Wu M, Yu H, et al. Isoliquiritin Ameliorates Cisplatin-Induced Renal Proximal Tubular Cell Injury by Antagonizing Apoptosis, Oxidative Stress and Inflammation. *Front Med Lausanne*. 2022;9:873739. doi:10.3389/fmed.2022.873739
49. Karadeniz A, Simsek N, Karakus E, et al. Royal jelly modulates oxidative stress and apoptosis in liver and kidneys of rats treated with cisplatin. *Oxid Med Cell Longev*. 2011;2011:981793. doi:10.1155/2011/981793
50. Liu X, Cai J, Jiao X, Yu X, Ding X. Therapeutic potential of mesenchymal stem cells in acute kidney injury is affected by administration timing. *Acta Biochim Biophys Sin*. 2017;49(4):338–348. doi:10.1093/abbs/gmx016
51. Srisawat N, Kellum JA. The Role of Biomarkers in Acute Kidney Injury. *Crit Care Clin*. 2020;36(1):125–140. doi:10.1016/j.ccc.2019.08.010
52. Ullah M, Liu DD, Rai S, Razavi M, Concepcion W, Thakor AS. Pulsed focused ultrasound enhances the therapeutic effect of mesenchymal stromal cell-derived extracellular vesicles in acute kidney injury. *Stem Cell Res Ther*. 2020;11(1):398. doi:10.1186/s13287-020-01922-1
53. Zheng J, Gao T, Shi H, Huang Y, Xiang Y, Li G. Electrochemical analysis of 8-hydroxy-2'-deoxyguanosine with enhanced sensitivity based on exonuclease-mediated functional nucleic acid. *Talanta*. 2019;199:324–328. doi:10.1016/j.talanta.2019.02.080
54. McSweeney KR, Gadanec LK, Qaradakhi T, Ali BA, Zulli A, Apostolopoulos V. Mechanisms of Cisplatin-Induced Acute Kidney Injury: pathological Mechanisms, Pharmacological Interventions, and Genetic Mitigations. *Cancers*. 2021;13(7):1572. doi:10.3390/cancers13071572
55. Akcay A, Nguyen Q, Edelstein CL. Mediators of inflammation in acute kidney injury. *Mediators Inflamm*. 2009;2009:137072. doi:10.1155/2009/137072
56. Singbartl K, Formeck CL, Kellum JA. Kidney-Immune System Crosstalk in AKI. *Semin Nephrol*. 2019;39(1):96–106. doi:10.1016/j.semnephrol.2018.10.007
57. Manganeli Polonio C, Longo de Freitas C, Garcia de Oliveira M, et al. Murine endometrial-derived mesenchymal stem cells suppress experimental autoimmune encephalomyelitis depending on indoleamine-2,3-dioxygenase expression. *Clin Sci*. 2021;135(9):1065–1082. doi:10.1042/cs20201544
58. Morigi M, Rota C, Remuzzi G. Mesenchymal Stem Cells in Kidney Repair. *Methods Mol Biol*. 2016;1416:89–107. doi:10.1007/978-1-4939-3584-0_5
59. Basile DP, Anderson MD, Sutton TA. Pathophysiology of acute kidney injury. *Compr Physiol*. 2012;2(2):1303–1353. doi:10.1002/cphy.c110041
60. Zhang R, Yin L, Zhang B, et al. Resveratrol improves human umbilical cord-derived mesenchymal stem cells repair for cisplatin-induced acute kidney injury. *Cell Death Dis*. 2018;9(10):965. doi:10.1038/s41419-018-0959-1
61. Manohar S, Leung N. Cisplatin nephrotoxicity: a review of the literature. *J Nephrol*. 2018;31(1):15–25. doi:10.1007/s40620-017-0392-z
62. Li J, Gui Y, Ren J, et al. Metformin Protects Against Cisplatin-Induced Tubular Cell Apoptosis and Acute Kidney Injury via AMPKα-regulated Autophagy Induction. *Sci Rep*. 2016;6(1):23975. doi:10.1038/srep23975
63. Ozkok A, Edelstein CL. Pathophysiology of cisplatin-induced acute kidney injury. *Biomed Res Int*. 2014;2014:967826. doi:10.1155/2014/967826
64. Fan M, Zhang J, Xin H, He X, Zhang X. Current Perspectives on Role of MSC in Renal Pathophysiology. *Front Physiol*. 2018;9:1323. doi:10.3389/fphys.2018.01323
65. Nakamae T, Adachi N, Kobayashi T, et al. The effect of an external magnetic force on cell adhesion and proliferation of magnetically labeled mesenchymal stem cells. *Sports Med Arthrosc Rehabil Ther Technol*. 2010;2(1):5. doi:10.1186/1758-2555-2-5